

# Cancerous Cells Targeting and Destruction Using Folate Conjugated Gold Nanoparticles

Ali Shakeri-Zadeh<sup>1</sup> • G. Ali Mansoori<sup>1\*</sup> • A. Reza Hashemian<sup>2</sup> • Hossein Eshghi<sup>3</sup> • Ameneh Sazgarnia<sup>2</sup> • A. Reza Montazerabadi<sup>2</sup>

<sup>1</sup> Department of Bioengineering, University of Illinois at Chicago, Chicago, IL, USA

<sup>2</sup> Department of Medical Physics, Mashhad University of Medical Sciences, Mashhad, Iran

<sup>3</sup> Department of Chemistry, Ferdowsi University, Mashhad, Iran

Corresponding author: \* mansoori@uic.edu

## ABSTRACT

We report here the production and use of a new nanoconjugate made up of folate and gold nanoparticle (AuNP) and conjugated by 4-aminothiophenol (4Atp), named Folate-4Atp-AuNP and applied for the selective cancer cells targeting and destruction. Its excellent selective cancer cells targeting capability is due to its folate segment. Its highly localized cell damage capability is because of photothermal treatment due to the presence of the gold nanoparticle, which can strongly absorb visible light and rapidly convert it into heat. The level of light-induced damage and cytotoxicity of the Folate-4Atp-AuNP nanoconjugate is investigated using MTT assay. Experiments are conducted on human adenocarcinoma HeLa cell chosen as the model cancer cell line because of its folate receptor overexpression (Masters 2002). In addition, MCF7 cell line was used as the “blank sample” because of its low level of folate receptor expression (Dickson *et al.* 1986). Identical Folate-4Atp-AuNP nanoconjugate concentrations, incubation periods and radiation exposure were used for both cell lines. The effect of light-gold nanoparticle interaction on cell lethality is examined and reported in detail. No significant cytotoxicity caused by the Folate-4Atp-AuNP nanoconjugate and cell damage induced by light was observed for both cell lines. Following photothermal treatment, more than 95% cell killing was achieved for HeLa cells whereas cell lethality for MCF7 was up to 26%. It was found that cell lethality depended strongly on incubation period and the nanoconjugate concentration. The cancerous cell targeting and destruction method described in this study is an effective photothermal cancer therapy technique, which can be effective for *in vivo* cancer therapy.

**Keywords:** 4-aminothiophenol, cancer, cell destruction, cell targeting, cytotoxicity, folate, folic acid, *folate-4Atp-AuNP*, folate receptor, gold nanoparticle, HeLa cell, intense pulsed light (IPL), MCF7 cell, nanoconjugate, nanophotothermolysis, nanotechnology, pteroyl-glutamic acid, photothermal treatment, targeted therapy

**Abbreviations:** **4Atp**, 4-aminothiophenol; **AuNP**, gold nanoparticle; **DCC**, *N,N*-dicyclohexylcarbodiimide; **DMSO**, dimethylsulfoxide; **FCC**, face centered cubic; **FCS**, fetal calf serum; **Folate-4Atp-AuNP**, folate-conjugated gold nanoparticle through 4-aminothiophenol; **FTIR**, Fourier transform infra red; **IPL**, intense pulsed light; **MCF7**, human, Caucasian, breast, adenocarcinoma; **MTT**, 3-[4,5-dimethylthiazol-2-yl]-2,5-diphenyltetrazoliumbromide; **TEM**, transmission electron microscopic; **XRD**, x-ray diffraction

## INTRODUCTION

Cancer is a disease of the cell in which the normal mechanisms of control of cell growth and proliferation are disturbed. Presently, several novel nanotechnology methods are under investigation and development for cancer therapy. Nanotechnology offers the opportunity to produce specific nanoparticles holding capabilities in cancer therapy. The synthesis of such nanoparticles with such particular properties has been the focus of extensive research over the past decade. Among these nanoparticles, gold nanoparticle (AuNP) are of major interest for developing unique systems with high potential for cancer treatment (Mansoori 2005; Mansoori *et al.* 2007a).

AuNP has represented a completely novel technology in the field of nanoparticle-based cancer therapy. AuNP has properties in absorption of light in the visible region, which makes it suitable for use in cancer photothermal treatment. The absorbed light by AuNP is rapidly converted into heat. In fact, AuNP atoms are excited to upper electronic states owing to absorption of photons. AuNP atoms decay to their ground state with effective electron-phonon conversion of the absorbed photon energy into thermal energy. Additionally, AuNP does not seem to possess any biologically harmful side- or after-effects (Jain *et al.* 2008).

Actually, when light pulses irradiate AuNPs, a process

named nanophotothermolysis occurs. In nanophotothermolysis, AuNPs heat up quickly because the absorbed light by the AuNP converts to heat on a picosecond time scale. Practically, AuNP strongly absorbs visible light irradiation. This absorbed energy transforms quickly into heat, which could cause fatal damage to cancer cells through local overheating effects. For example, a 30-nm AuNP irradiated by a laser pulse ( $\lambda = 532$  nm; fluence =  $0.5$  J/cm<sup>2</sup>) could produce a temperature in the order of 2500 K at the end of a 20 nanosecond pulse (Zharov *et al.* 2003). The high temperature produced by AuNPs can be controlled to kill cancerous cells. Accordingly, AuNPs are potentially very practical and efficient photothermal agents in therapeutic applications, especially in cancer treatment (Mansoori *et al.* 2007b).

The photothermal properties of AuNP are indicative of the fact that if AuNPs enter cancerous cells, they will cause photothermal effects after irradiating by an appropriate light source. However, it is important to prevent AuNPs from entering normal cells during such irradiation by the visible light. As a result, it is necessary to design AuNPs that will target cancerous cells selectively. Nanotechnology-based targeting of cancer cells is the main approach to meet this goal. In the present report we use folic acid as the targeting agent attached to AuNP and we specifically target folate receptor binding sites on the surface of cancer cells.

Folic acid is one of the materials which can be applied

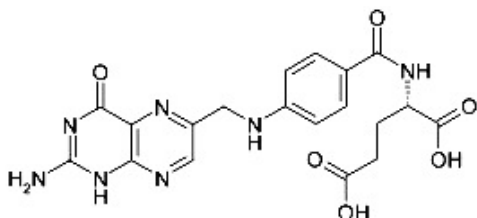


Fig. 1 The chemical structure of folic acid (pteroylglutamic acid).

as targeting agents for therapeutic purposes (Sudimack and Lee 2000). Folic acid is also named pteroylglutamic acid and has the closed chemical formula  $C_{19}H_{19}N_7O_6$  (MW = 441.4 Da) and open chemical structure as shown in Fig. 1.

Folic acid is a well-known water-soluble vitamin of the B-complex group. Folate, the folic acid salt, or pteroylglutamate, is also water-soluble. Folate is found in leafy vegetables and the name comes from the Latin word "*folium*" meaning leaf. It is an important vitamin required for the healthy functioning of all cells. Specifically, folate is necessary for the DNA nucleotide synthesis and cell division. Folate is brought into, both, healthy and cancerous cells by the folate receptor. Folic acid (or folate, the folic acid salt or pteroylglutamate) specifically binds with a folate receptor existing on the surface of tumoral cells. It is a stable, inexpensive, and non-immunogenic chemical, and has a high affinity as a cell surface receptor. Actually, folate is important for the healthy functioning of all cells, but cancer cell will require much more folate than a healthy cell.

Folate receptor with an apparent molecular weight of 38–40 kDa binds folic acid with high affinity. Folate receptor is a glycosylphosphatidylinositol-linked membrane glycoprotein and is known as the high-affinity membrane folate-binding protein. The family of human folate receptors consists of three well-characterized isoforms, FR- $\alpha$ , FR- $\beta$ , and FR- $\gamma/\gamma'$ . These three folate receptors are about 70–80% the same in their amino acid sequences, but they are different in their expression patterns (Antony 1996). The presence of the folate receptors on a cell surface is regulated by the cell function. Folate receptor transports folate into the cytosol of the cell for the synthesis of thymine by dihydrofolate reductase. Nearly all cells express the folate receptor, for normal DNA replication as well as cell division, however cancerous cells express a much greater amount of folate receptors (500+ times more than healthy cells). Cancer cells overexpress the folate receptor because of their vast requirement for folate. As a result, the high affinity of folic acid and folate for folate receptors provides a unique opportunity to use it as a targeting ligand to deliver nanoparticles to cancer cells (Doucette and Stevens 2001). Because of the low expression level of folate receptor in healthy cells and its overexpression in cancerous tissues, folate behaves as a suitable targeting agent as it is utilized in this research.

We report here the results of our research on: i) production of AuNPs, ii) Synthesis of Folate-4Atp-AuNP which is a result of conjugation of AuNP with folate by 4-aminothiophenol (4Atp), iii) Targeting of cancer cells by taking advantage of the cancer cells' folate receptor appetite for folate and iv) destruction of cancer cells through nanophotothermolysis of AuNP.

## MATERIALS AND METHODS

### Materials

The chemical and biological compounds used in this research are as follows: Hydrogen tetrachloroaurate (III) trihydrate ( $H AuCl_4 \cdot 3H_2O$ , 99.5 % purity), 4-aminothiophenol ( $C_6H_7NS$ , 95% purity), sodium borohydride ( $NaBH_4$ , 99.99% purity), and N, N'-dicyclohexylcarbodiimide ( $C_{13}H_{22}N_2$ , >99% purity) all were purchased from Merck, Germany. Folic acid ( $C_{19}H_{19}N_7O_6$ , 97% purity) was purchased from Fluka, Switzerland. Trypan blue, RPMI 1640, MTT (3-[4,5-dimethylthiazol-2-yl]-2,5-diphenyltetra-

zoliumbromide), dimethylsulfoxide (DMSO), streptomycin, penicillin and trypsin-EDTA were purchased from Sigma (St. Louis, MO, USA). Fetal calf serum (FCS) was purchased from Gibco (Merelbeek, Belgium). HeLa and MCF7 cell lines were obtained from the Pasteur Institute of Iran.

### Preparation of gold nanoparticles conjugated with 4-aminothiophenol (4Atp-AuNP)

A solution of  $H AuCl_4 \cdot 3H_2O$  (40 mg, 0.1 mM) in  $CH_3OH$  (10 mL) was added to a stirred solution of 4-aminothiophenol (4Atp, 75 mg, 0.6 mM) in  $CH_3OH$  (10 mL). After 20 min of stirring, a freshly prepared solution of sodium borohydride (57 mg, 1.5 mM) in deionized water (5 mL) was added to the vigorously stirred reaction mixture drop-wise in a 15 min period. The reaction mixture turned deep brown indicating the formation of AuNPs. The stirring was continued for 1 hr. Finally, the conjugation of AuNP and 4Atp were separated from methanol by precipitation under centrifuge at 10,000 rpm and purified by successive washing with  $CH_2Cl_2$  and deionized water. Ultrasound sonication was performed to disperse the nanoparticles into the base material thoroughly. Subsequently, centrifuging and washing with deionizer water was carried out to reach additional purification. We obtained the conjugation of 4Atp-AuNP after drying and the results were stored for further characterization and reactions.

### Preparation of folate-conjugated gold nanoparticle (Folate-4Atp-AuNP)

A solution of folic acid (22 mg, 0.05 mM) in DMSO (5 mL) was added to pre-sonicated colloids of 4Atp-AuNP (8 mg) in  $CH_2Cl_2$  (10 mL). The orange mixture that resulted was vigorously stirred for 20 min. After this time, a solution of N,N'-dicyclohexylcarbodiimide (DCC) (11 mg, 0.05 mM) in  $CH_2Cl_2$  (10 mL) was added to the orange mixture drop-by-drop while stirring. The stirring was continued for ten hours and a green-color mixture was obtained. The final product was separated by fast centrifugation. It was subsequently washed with  $CH_2Cl_2$ . To obtain more purification, ultrasound sonication was carried out and then the mixture was centrifuged and washed with deionized water again. The final product (Folate-4Atp-AuNP) was obtained as a powder after drying. This powder exhibited a golden color in reflection.

### Characterization techniques

UV-visible (UV-vis) absorption spectroscopic measurements were recorded on a single beam UV-vis spectrometer, Agilent 8453, using quartz cells of 1 cm path length and methanol as the reference solvent at room temperature. Also, Fourier Transform Infra Red (FTIR) measurements were recorded on a Shimadzu FT-IR 4300 instrument using KBr pellets at room temperature. Transmission electron microscopic (TEM) images of the nanoparticles were taken with a LEO 912AB instrument operated at an accelerating voltage of 120 kV with line resolution of 0.3 nm at room temperature. The samples for TEM measurements were prepared by placing a droplet of the colloidal solution onto a carbon-coated copper grid and allowing it to dry in air naturally. X-ray diffraction (XRD) was carried out with a Bruker D8 ADVANCE X-ray Diffractometer, using the wavelength of 0.15406 nm ( $CuK\alpha$ ) radiations at room temperature. Based on the TEM images we determined the size distributions of the final product by counting at least 300 particles. The elemental analyses for carbon, hydrogen, nitrogen, sulfur and oxygen were performed using a Thermo Finnigan Flash EA CHNS-O analyzer. We determined the gold percentage in the Folate-4Atp-AuNP by Shimadzu model AA-670 atomic absorption spectrophotometer.

### Cell culture

HeLa and MCF-7 cells both were grown continuously as a monolayer using RPMI 1640 with L-glutamine and  $NaHCO_3$  supplemented with 10% FCS, penicillin (100 U/mL), and streptomycin (100  $\mu$ g/mL) in 175  $cm^2$  flasks (BD-Falcon, BD Biosciences, MA, USA). Cell growth was carried out in a humidified atmosphere containing 5%  $CO_2$ -95% air at 37°C. Culture medium was

changed every second day until a sufficient number of cells were obtained.

### Light source

In this study, an intense pulsed light (IPL) source (Lumenis Ltd.) was used as the light source. IPL is a noncoherent, broad-spectrum light emitted from a flash lamp. The equipment used in this research has the following properties. It provides IPL with a continuous light spectrum with most of its energy at wavelengths between 515 and 1,200 nm. The pulse durations range between 3-100 milliseconds per pulse. The energy fluence range varies between 10-40 J/cm<sup>2</sup> in one pulse sequence. Operating modes are single, double or triple pulses in each pulse sequence. The spot size is larger than that of other lasers with an illuminated area of 8 mm × 15 mm. The optical energy is directly coupled through a light guide. All settings are computer controlled.

In our research, studies were made with energy of 15 J/cm<sup>2</sup>, cut-off filter of 560 nm, pulse duration of 3 milliseconds and single pulse. These treatment parameters were chosen according to the results obtained based on our primary studies as pilot. To find the effects of IPL exposure to cells, different pulse numbers (10, 15, 20, 30, and 40 pulses) were applied to, both, HeLa and MCF7 cell lines.

### Cytotoxicity assay

When the cells reached more than 85% confluence, they were washed with trypsin-EDTA solution for 10 min at 37°C to remove adherent cells from a culture flask surface. Cells were then resuspended in media, centrifuged (at 1200 rpm for 5 min) and the cells were counted through staining with trypan blue for seeding cell density and to ensure viability. Nanoconjugates at different concentrations (1, 5, 15, 20, 100 µg/mL) dispersed in deionized water were incubated with the density of 10<sup>6</sup> cells/mL for different incubation periods (1, 2, 4 h). The same density of cells was considered with out nanoconjugates as the control group. When the incubation time was over, the cells were centrifuged at 1200 rpm for 5 min. After that, the incubated cells were separated and plated at a density of 5000 cells/well in flat-bottom 96-well plates.

IPL irradiation to each well was separately performed at the fluence of 15 J/cm<sup>2</sup> using 20 pulses for each treatment or control group. The light spot covered 1 well which was considered as one experimental group. Following photothermal treatment, the cells

were located to the incubator overnight. It should be noted that sufficient control groups were considered for nanoconjugate and light exposure, separately.

Cell viability was estimated by the MTT-tetrazolium assay based on the ability of metabolically active mitochondria of live cells. Accordingly, culture medium was removed from 96-well plate. Followed by adding 100 µL culture medium without FCS, 10 µL MTT were added to each well and the plate was returned to incubator for 4 hrs. After 4 hrs, culture media was removed from wells and cells were lysed in 200 µL of DMSO. After formazan was dissolved, the absorbance at the wavelength of 545 nm was read on an ELISA reader (Stat Fax-2100 Awareness, Mountain View, CA, USA). Relative survival was represented as the absorbance of treated sample/absorbance of control group. Eight replicates were used for each condition. All experiments were repeated at least three times.

### Statistical analysis

The SPSS package (SPSS Inc., Chicago, IL, USA) for Windows<sup>®</sup> version 12.0 was used to analyze the data. The generation of survival curves was performed using the Microsoft Office Excel. Normality of distribution was assessed using the Kolmogorov-Smirnov Test. Data were analyzed for statistical differences ( $P < 0.05$ ) using one-way ANOVA followed by Tukey's multiple comparison test for comparison of all groups.

### CHARACTERIZATION OF FOLATE-CONJUGATED GOLD NANOPARTICLES

Considering the folate receptor targeting capability joined with the optical properties of AuNPs in cancer photothermal treatment, we have developed a targeted therapy technique by attaching AuNPs to folate molecules (Eshghi *et al.* 2008). In order to conjugate an AuNP with a folate we first synthesized appropriate AuNPs as discussed above. Since the gold surface preferentially binds to the thiol's-SH functional group (Johnson *et al.* 1998) we selected an appropriate thiol derivative compound as a linker between the AuNP and folate. This bifunctional linker has the capability to conjugate simultaneously with AuNPs and folate molecule from its two separate ends.

We synthesized AuNPs according to the standard wet chemical methods (Smith and March 2007) using sodium

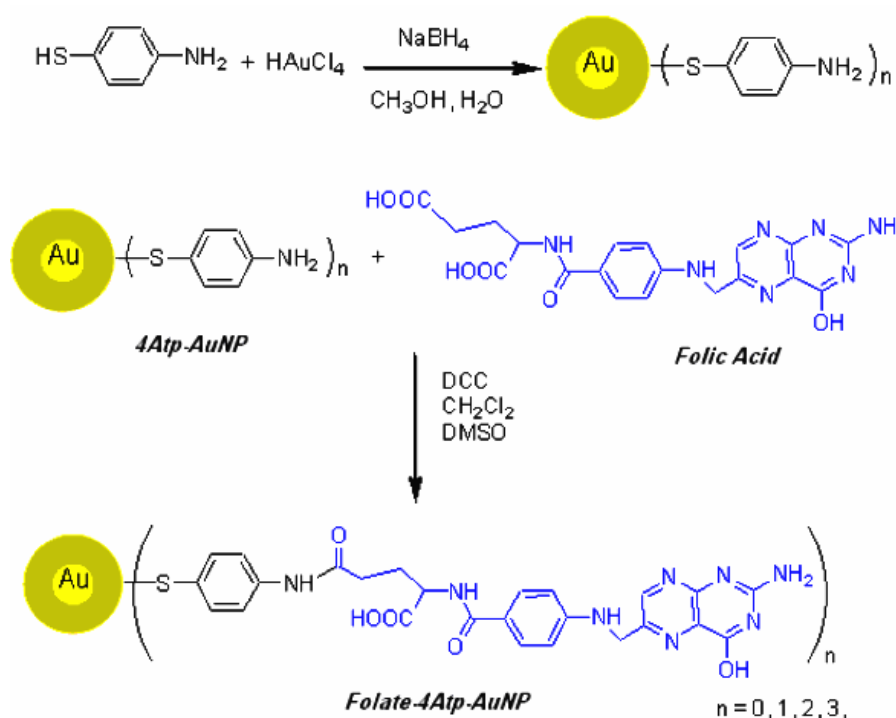


Fig. 2 Scheme for the synthesis procedure of folate conjugated with AuNP with 4-aminothiophenol (4Atp) as the connecting medium to produce Folate-4Atp-AuNP nanoconjugate.

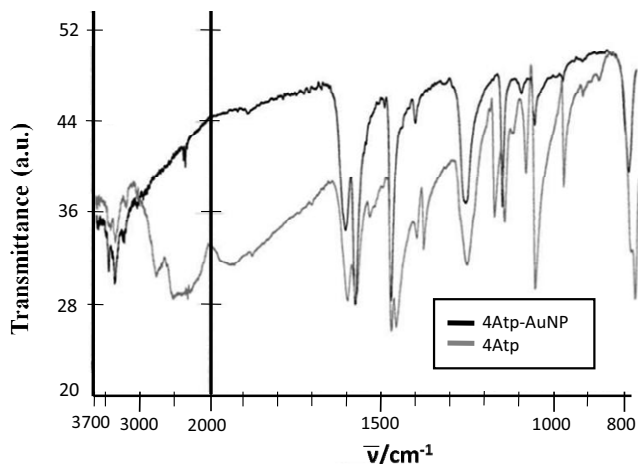


Fig. 3 FTIR spectra of 4Atp-AuNP in comparison to 4Atp.

borohydride,  $\text{Na}^+ [\text{H}_4\text{Br}]$ , as a reducing agent. Folate-conjugated AuNPs were prepared using 4-aminothiophenol (4Atp) as the linker as shown in Fig. 2 (Eshghi *et al.* 2008).

4Atp reacts with hydrogen tetrachloroaurate ( $\text{HAuCl}_4$ ) in aqueous methanol solution at room temperature to produce dark brown 4Atp-stabilized gold nanoparticles (4Atp-AuNP). In this conjugation, 4Atp as a bidentate spacer attaches to the AuNP via its sulfur atom. 4Atp has been selected for binding to AuNP because it is  $-\text{SH}$  terminated and its oxidation in the attachment to AuNP is well known (Smith and March 2007). There is also a  $-\text{NH}_2$  group at the other end of 4Atp molecule, which is suitable for conjugation to folate. Our preference for the choice of amide bond formation in the attachment of folate to AuNP is its stronger bond as compared to other linkers such as thioesters (Carey and Sundberg 2007). Ester and thioester hydrolysis may be problematic in the physiologic transfer of drug to the target cells.

Because of the bonding procedure mentioned above we obtained the folate conjugated gold nanoparticles (Folate-4Atp-AuNP for short) as shown in Fig. 2, which is a clean colloid with green color in macroscopic quantities. Folate-4Atp-AuNP was then separated and precipitated through centrifugation. We clearly identified the formation of such conjugations from their UV-visible and FTIR spectra as described below.

Fig. 3 shows the FTIR spectrum of 4Atp-AuNP as compared with the spectrum of neat 4Atp. According to this Figure, the infrared spectrum of 4Atp-AuNP shows the characteristic bands of  $-\text{NH}_2$  group in  $3440$  and  $3325 \text{ cm}^{-1}$  wavenumbers. With regard to the spectrum of 4Atp-AuNP in comparison to the spectrum of 4Atp, it can be found that the  $-\text{SH}$  stretching vibration ( $2560 \text{ cm}^{-1}$ ) has disappeared. As a result, the formation of S-Au bond can be inferred because significant changes in many characteristics of thiol vibrations have been occurred. In addition, the intensity of some of the vibrations in the fingerprint region has been decreased or disappeared. These all confirm that the bonding of 4Atp to the AuNP surface has been taken place through the  $-\text{SH}$  group.

AuNPs possess the characteristic surface plasmon absorption at  $520 \text{ nm}$  in the UV-visible absorption spectrum. This characteristic absorption band in the assemblies of AuNPs interlinked by various molecules exhibit a peak between  $520$  and  $620 \text{ nm}$ . Because of the propensity for intermolecular hydrogen bonding in the assemblies of AuNPs interlinked by different ligands, resultant broadening and red-shifting of the plasmon absorption peak are to be expected. It is worthy to note that this is the most prominent in the case of assemblies of AuNPs interlinked by 4Atp. Also,  $\lambda_{\text{max}}$  of these assemblies (AuNPs-Ligands) is dependent on the particle size. Accordingly, a significant broadening of the gold surface plasmon bands or the appearance of a red-shifted absorption band due to coupling of the individual

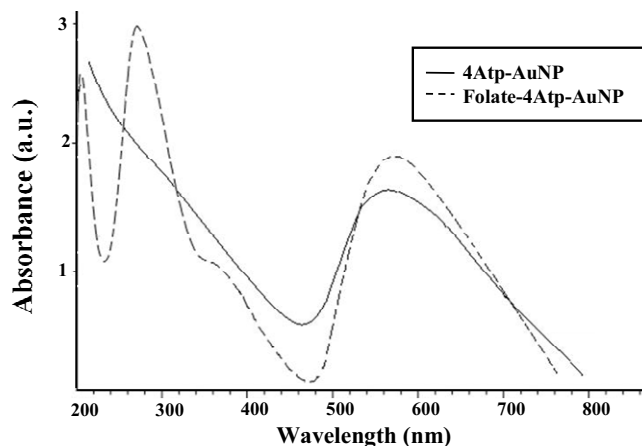


Fig. 4 UV-Visible absorption spectra of 4Atp-AuNP and Folate-4Atp-AuNP conjugated gold nanoparticles.

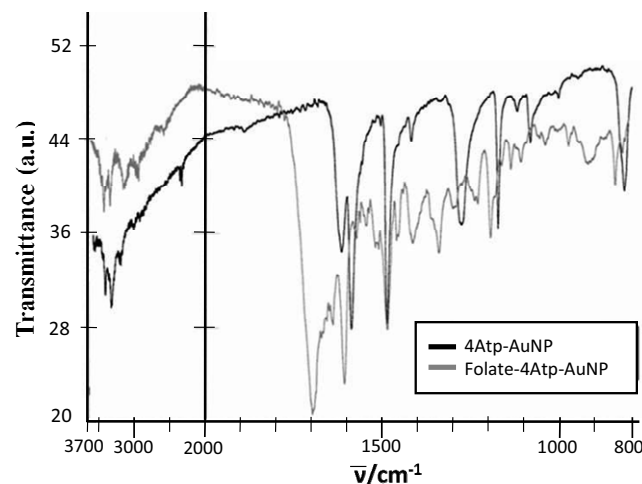


Fig. 5 FTIR spectra of Folate-4Atp-AuNP in comparison to 4Atp-AuNP.

surface plasmon of nanoparticles in the aggregated structures will be observed if the interlinked nanostructures are formed (Link and El-Sayed 1999; Pan *et al.* 2003; Smith and March 2007).

Fig. 4 shows the UV-vis spectra of the synthesized 4Atp-AuNP and Folate-4Atp-AuNP conjugated AuNP.

In the spectrum of 4Atp-AuNP the appearance of surface plasmon bands around  $560 \text{ nm}$  confirms the formation of stable AuNP. Moreover, according to Zhang *et al.* (2003) the absorption maxima at  $280$  and  $360 \text{ nm}$  can be used for confirming the covalent attachment of the folate with Atp-AuNP. According to this figure, it can be seen that the Folate-4Atp-AuNP nanoconjugate has three absorption peaks in UV-visible wavelengths. By studying the UV-Visible absorption spectrum, we determined that Folate-4Atp-AuNP has the absorption peaks at  $275 \text{ nm}$  and  $362 \text{ nm}$  pertaining to folate and absorption peak at  $564 \text{ nm}$  pertaining to AuNP. Based on this data we selected the  $560 \text{ nm}$  filter of IPL device for irradiating our samples.

Fig. 5 shows the FTIR spectra of Folate-4Atp-AuNP in comparison to 4Atp-AuNP. According to Fig. 5, the FTIR spectrum of Folate-4Atp-AuNP shows the strong carbonyl absorbance at  $1700 \text{ cm}^{-1}$  due to  $-\text{CONH}-$  and  $\alpha\text{-COOH}$  groups stretching of folate conjugate. In addition, the bands at  $3500$ ,  $3375$ , and  $3200 \text{ cm}^{-1}$  correspond to the  $\text{NH}_2$  and amide  $\text{NH}$  stretches of folate conjugate, respectively. Additionally, the bands at  $835$ ,  $1190$ , and  $1290 \text{ cm}^{-1}$  correspond to the out-of plane and in plane motions of  $\text{NH}_2$ , and C-N stretch of folic acid (not shown) and 4Atp-AuNP conjugate are shifted to  $855$ ,  $1220$ , and  $1320 \text{ cm}^{-1}$ , respectively. These all indicate the formation of folate conjugation in the Folate-4Atp-AuNP.

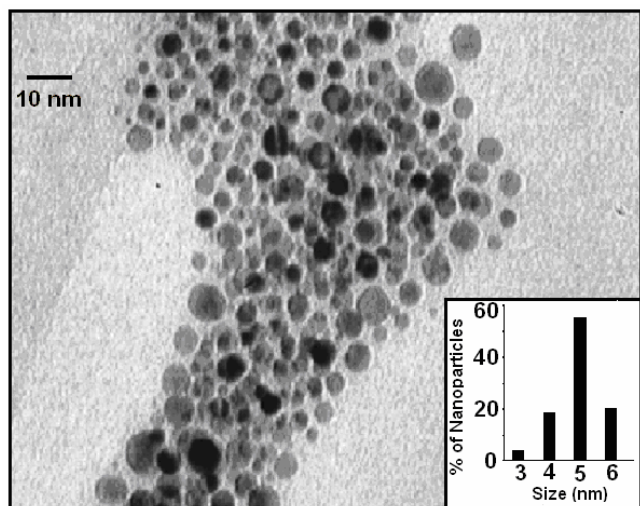


Fig. 6 TEM photograph of Au nanoparticles in Folate-4Atp-AuNP nanoconjugate and histogram for the size distribution of Au nanoparticles.

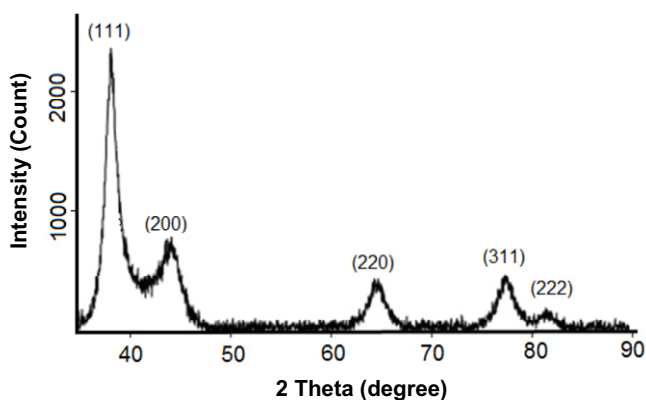


Fig. 7 XRD pattern of Au nanoparticles in Folate-4Atp-AuNP.

Elemental analysis of Folate-4Atp-AuNP determined by carbon hydrogen nitrogen sulfur oxygen (CHNS-O) analysis and atomic absorption spectrometry resulted in [C] = 28.7%, [H] = 2.5%, [N] = 13.3%, [S] = 3.5%, [Au] = 41.3% and [O] = 10.7%. The [C]: [H] = 11.48 and [S]: [H] = 1.4 ratios are within the experimental uncertainties, equal to those of the Folate-4Atp conjugate.

We also report the transmission electron microscopic (TEM) micrograph of the synthesized Folate-4Atp-AuNP and the size histogram of the Folate-4Atp-AuNP nanoparticles determined by counting at least 300 particles in Fig. 6.

According to Fig. 6 the shape of nanoparticles is quite spherical and the size histogram indicates the formation of nearly monodispersed nanoparticles with an average diameter of 5 nm.

As shown in Fig. 7, the crystalline nature of these nanoparticles is confirmed through the X-ray diffraction (XRD) analysis, where (111), (200), (220), (311), and (222) crystal planes of metallic face-centered cubic (fcc) structure are identified with a lattice constant of 0.407376 nm.

### In vitro tests of folate-4Atp-AuNP nanoconjugate on cancer cells

The folate-conjugated gold nanoparticle (Folate-4Atp-AuNP) designed and reported by Fig. 2 is used to selectively target the folate receptor that is overexpressed on the surface of tumoral cells. In this section we report the result of our study of utilizing Folate-4Atp-AuNP for the improvement of cellular internalization of AuNP. For this purpose, human adenocarcinoma HeLa cells are chosen as our model cancer cell line because it is known this cell line

overexpress folate receptors outside its membrane (Masters 2002). HeLa cell is an immortal cell line used in medical research, which was derived from cervical cancer cells. In addition, MCF7 cell line is selected as the blank test because of its very low level of folate receptor expression (Brooks *et al.* 1973). The MCF-7 cell line, isolated from a pleural effusion of a 69-years-old Caucasian women with breast carcinoma. Actually, in this research, preferential targeting to cancerous cells by Folate-4Atp-AuNP is studied by comparing the results obtained from HeLa and MCF7 cell lines.

### Nanoparticle cytotoxicity

We investigated the cytotoxicity effects of the Folate-4Atp-AuNP nanoconjugate on HeLa and MCF7 cell lines at various concentrations ranged from 1 to 100  $\mu\text{g/mL}$ . Excess cytotoxicity was investigated for different incubation periods of 1, 2 and 4 hrs. Experiments performed on nanoconjugate dispersed in deionized water led to quite similar results, after incubation with both HeLa and MCF7 cells. The results achieved by performing cytotoxicity tests on HeLa and MCF7 cells are shown in Figs. 8 and 9, respectively. According to Fig. 8 no significant cytotoxicity was observed even at the higher nanoparticles concentrations (100  $\mu\text{g/mL}$ ) for HeLa cells which are folate receptor over-expressed.

It can be seen from Fig. 9 the Folate-4Atp-AuNP nanoconjugate has also no significant cytotoxicity on MCF7 cells, which possess low level of folate receptor expression.

Overall, no significant cytotoxicity difference was observed between HeLa and MCF7 cell lines as it is evident from Fig. 8 and Fig. 9.

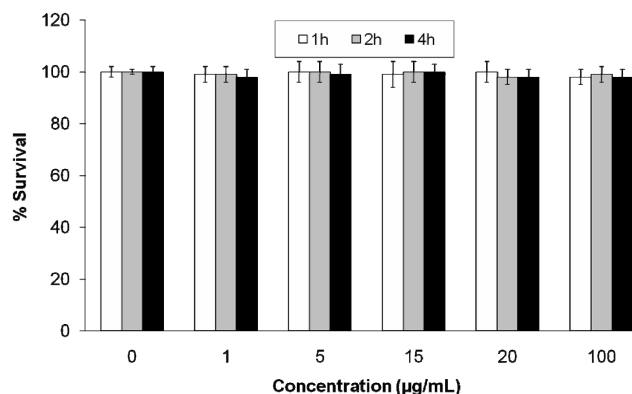


Fig. 8 The percentage of survival for HeLa cells incubated with different concentrations of Folate-4Atp-AuNP nanoconjugate for 1, 2, and 4 hours of incubation times.

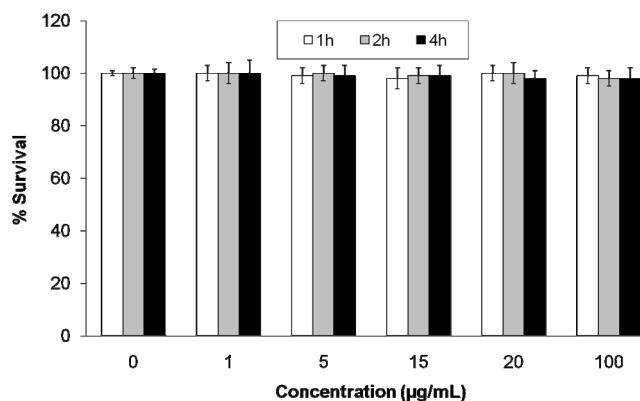


Fig. 9 The percentage of survival for MCF7 cells incubated with different concentrations of Folate-4Atp-AuNP nanoconjugate for 1, 2, and 4 hours of incubation times.

## Effects of intense pulsed light (IPL) exposure to cells

To examine the effect of IPL on HeLa and MCF7 cell lines, different pulse numbers were applied to both cell lines without the presence of nanoconjugate. These examinations were conducted to observe how the number of pulses changes the percentage of cell survival. For this purpose, the parameters of each pulse were selected based on the procedure described above. **Light source.** Fig. 10 shows the results of our *in vitro* studies on HeLa and MCF7 cell lines using IPL probe without the presence of Folate-4Atp-AuNP nanoconjugates.

According to Fig. 10 no significant cell lethality took place when the number of pulses, with the specified properties, was increased up to 20 pulses. The percentage of HeLa cells viability from  $(98 \pm 2)\%$  for 20 pulses dropped off to  $(71 \pm 4)\%$  for 30 pulses and to  $(45 \pm 4)\%$  for 40 pulses. The percentage of MCF7 cells viability from  $(98 \pm 2)\%$  for 20 pulses dropped off to  $(75 \pm 3)\%$  for 30 pulses and to  $(54 \pm 4)\%$  for 40 pulses.

Based on the data presented in Fig. 10, it can be concluded that IPL exposure to both cell lines is harmless when up to 20 pulses are applied with specifications described. As a result, we conducted our later experiments using IPL with the same properties as reported in Figure 10, i.e.: Operating mode: single; Spot size: 8 mm × 15 mm; Fluence: 15 J/cm<sup>2</sup>; Filter (wavelength): 560 nm; Pulse duration: 3 milliseconds; Number of pulses: 20}.

## Photothermal studies

As noted in the Introduction of this report AuNPs in the presence of appropriate light irradiation produce high temperatures. The level of temperature produced by AuNPs impregnated inside cancerous cells can be controlled by the level and duration of radiation in order to photothermally kill the cells. We have investigated the potential of the Folate-4Atp-AuNP nanoconjugate, which we have produced for photothermal treatment using an IPL probe. We have also investigated the differences between using the Folate-4Atp-AuNP nanoconjugate along with IPL exposure for the HeLa cell line, which is folate receptor overexpressed and the MCF7 cell line, with low level of folate receptors.

In all of our *in vitro* experiments the IPL pulse duration was kept at 3 milliseconds. We investigated the role of two factors on photothermal treatment of cells: 1. the effect of the dosage of Folate-4Atp-AuNP nanoconjugate on photothermal treatment; 2. the effect of incubation period of cells with Folate-4Atp-AuNP nanoconjugate. In Fig. 11 we report the percentages of survival of HeLa cells incubated with 0, 1, 5, 15, 20 and 100 µg/mL of the Folate-4Atp-AuNP nanoconjugate for 1, 2 and 4 hours of incubation.

According to Fig. 11 for the same incubation period the percentage of live HeLa cells is dependent on the dosage of the Folate-4Atp-AuNP nanoconjugate up to a dosage of 5 µg/mL. No significant difference is observed when the dosage of Folate-4Atp-AuNP nanoconjugate is above 5 µg/mL regardless of the Folate-4Atp-AuNP nanoconjugate concentration and the incubation period.

The most significant cell death at a minimum of nanoconjugate concentration occurred at 4 hours of incubation time and at 5 µg/mL nanoconjugate concentration. Specifically during 4 hours of incubation the viability of HeLa cells decreased from  $(98 \pm 1.6)\%$  at 1 µg/mL of nanoconjugate concentration to  $\sim 1\%$  at 5 µg/mL of nanoconjugate concentration.

It should be also pointed out that with one hour of incubation, the nanoconjugate concentration played a role in inducing cell death for up to the concentrations of 15 µg/mL of nanoconjugate. Concentrations >15 µg/mL did not seem to induce more cell lethality. The fastest decrease in cell viability was observed by using 5 µg/mL of nanoconjugate concentration and changing the exposure time from 1 hr  $(77 \pm 3)\%$  to 2 hrs  $(29 \pm 3)\%$ .

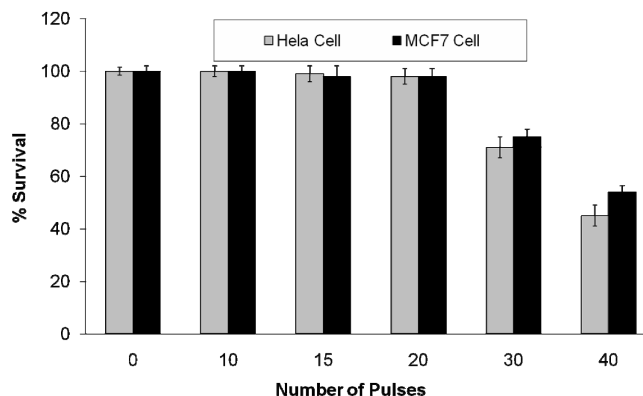


Fig. 10 The percentage of survival for HeLa and MCF7 cell lines obtained following exposing by different number of IPL pulses and the following properties: Operating mode: single; Spot size: 8 mm × 15 mm; Fluence: 15 J/cm<sup>2</sup>; Filter (wavelength): 560 nm; Pulse duration: 3 milliseconds.

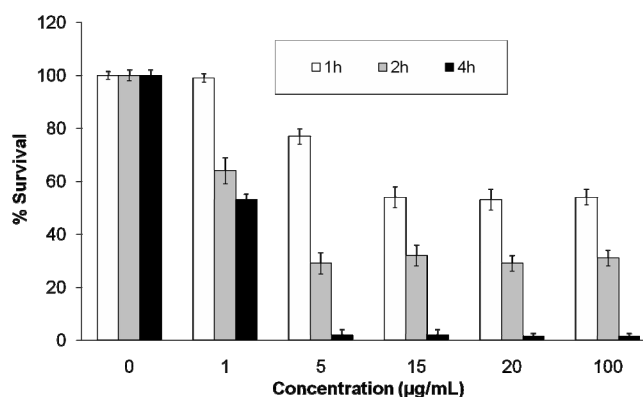


Fig. 11 The percentage of survival for HeLa cells obtained following photothermal treatment versus the Folate-4Atp-AuNP nanoconjugate concentration and at various incubation periods.

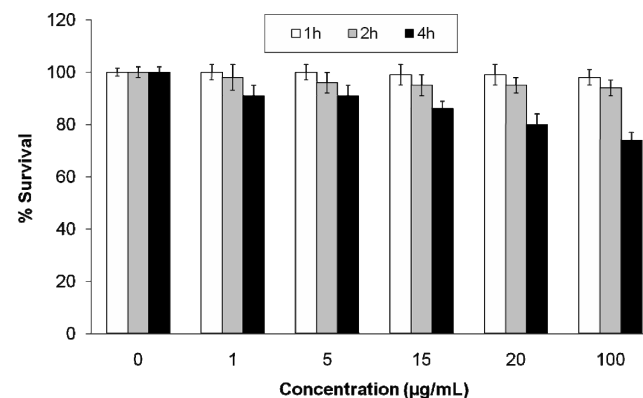


Fig. 12 The percentage of survival for MCF7 cells obtained following photothermal treatment.

Generally, to reach a higher level of cell death, longer incubation time is preferred over using higher concentrations of nanoconjugate. For example, according to Fig. 11, using 1 µg/mL of nanoconjugate incubated with HeLa cells for 4 hrs and 15 µg/mL of nanoconjugate incubated with HeLa cells for one hour induce a similar cell death.

To compare the amount of cell lethality observed for HeLa cells with MCF7 cells, additional experiments were conducted. This step of the research is designed to investigate whether nanoconjugates would operate selectively. Fig. 12 shows percentage of survival of MCF7 cells incubated with 1, 5, 15, 20, 100 µg/mL of nanoconjugate for different incubation time.

All the conditions for experiments on MCF7 cells were

identical to the conditions for experiments on HeLa cells. According to **Fig. 12** after one hour of incubation, no significant effects were observed for MCF7 cells even at very high concentrations (100  $\mu\text{g/mL}$ ) of nanoconjugate. The percentage level of MCF7 cells survival did not significantly alter by increasing the period of incubation time up to 2 hrs. Somewhat more cell death was observed in all concentrations for 4 hrs incubation. When the concentration increased from 1-100  $\mu\text{g/mL}$ , lethality in MCF7 cells varied at most from 9% (at 1  $\mu\text{g/mL}$  nanoconjugate concentration) to 26% (at 100  $\mu\text{g/mL}$  nanoconjugate concentration).

It is well-known that the level of folate receptor expression outside the cell membrane plays an effective role on the amount of nanoconjugates internalized into the cell. This means that a cell with high level of folate receptor expression on its surface can uptake higher amount of folate conjugated materials than a cell with low level of folate receptor expression. HeLa cells have significantly more folate receptors than MCF7 cells (Dickson *et al.* 1986; Masters 2002). Accordingly, it is expected that in the same concentration of nanoconjugate and incubation time, HeLa cells can uptake more nanoconjugates than MCF7 cells. As a result, if similar conditions of light exposure apply to both cell lines, HeLa cells lethality is higher than MCF7 cells.

By comparing **Fig. 11** and **Fig. 12**, we recognize a significant difference in the viability of HeLa and MCF7 cell lines. For example, 5  $\mu\text{g/mL}$  of nanoconjugate incubated with HeLa cell for 4 hours can induce cell lethality of (98  $\pm$  2)%, whereas cell lethality of (9  $\pm$  4)% can be achieved if the same conditions considered for MCF7 cells. This translates to a HeLa cell lethality of about 90%.

## CONCLUSION

We report the synthesis and characteristics of a new folate-conjugated gold nanoparticles using 4-aminothiophenol (4Atp) as a linker. UV-visible and FTIR spectroscopy confirms the attachment of folic acid to the AuNP. We confirm the crystalline nature of the final nanoconjugate product (Folate-4Atp-AuNP) by TEM micrographs and XRD spectroscopy. The conjugations of organic chains (Folate-4Atp) with AuNPs are confirmed using the data obtained from CHNS-O analysis and Au atomic absorption spectrometry.

Because this new synthesized complex nanoconjugate material (Folate-4Atp-AuNP) contains folate, it can be applied to selective targeting of folate receptor positive cancerous cells, which overexpress folate receptor on their surface. Significant absorption of this new synthesized complex makes it a promising material for using in the area of cancer therapy and thermal ablation of tumors.

We have experimentally demonstrated a method for selective nanophotothermolysis using folate conjugated AuNP. The method is used for HeLa and MCF7 cell lines, the former is used as overexpressed folate receptor cell and the later is used as the blank test cell. IPL is used to heat up the Folate-4Atp-AuNP nanoconjugate and good results were obtained.

The experimental results have lead to the following conclusions:

- Different concentrations of Folate-4Atp-AuNP nanoconjugate induced no significant cytotoxicity in both HeLa and MCF7 cells. As a result, it is concluded that the nanoconjugate is safe to cells even for long period of incubation time such as 4 hrs.
- Intense pulsed light (IPL) exposure to both HeLa and MCF7 cell lines partially impregnated with AuNP is found to be safe for cells not impregnated with AuNP according to the procedure introduced here.
- Gold nanoparticles (AuNPs) can be heated up to a desired temperature level through exposure to IPL ac-

ording to the procedure introduced in this report.

- Results from our studies showed that the *Folate-4Atp*-AuNP nanoconjugate concentration plays an important role in the photothermal cell destruction.
  - Our findings showed the process of the *Folate-4Atp*-AuNP nanoconjugate entering into the cells is strongly time-dependent.
  - Damage (cell lethality) of more than 90% for HeLa cells was achieved.
  - HeLa cell death due to photothermal treatment depends on the *Folate-4Atp*-AuNP nanoconjugate concentration and incubation time factors. MCF7 cell lethality is little dependent on the same factors.
  - It is found that HeLa cells lethality due to photothermal treatment will vary from 2-98%, while MCF7 cells lethality will vary from 1-26%.
- Overall, the procedure developed in this study can also be applicable for *in vivo* cancer therapy.

## REFERENCES

- Antony AC (1996) Folate-receptors. *Annual Review of Nutrition* **16**, 501-521
- Brooks SC, Locke ER, Soule HD (1973) Estrogen receptor in a human cell line (MCF-7) from breast carcinoma. *The Journal of Biological Chemistry* **248**, 6251-6253
- Carey FA, Sundberg RJ (2007) *Advanced Organic Chemistry* (5<sup>th</sup> Edn), Springer, NY, Part 1
- Cullity BD (1978) *Elements of X-ray Diffraction* (2<sup>nd</sup> Edn), Addison-Wesley, London, pp 101-102
- Dickson RB, Bates SE, Manaway MC, Lippman ME (1986) Characterization of estrogen responsive transforming activity in human breast cancer cell lines. *Cancer Research* **46**, 1707-1713
- Doucette MM, Stevens VL (2001) Folate receptor function is regulated in response to different cellular growth rates in cultured mammalian cells. *Journal of Nutrition* **131**, 2819-2825
- Hashemia A, Eshghi H, Mansoori GA, Shakeri-Zadeh A, Mehdizadeh A (2010) Folate-conjugated gold nanoparticles. Synthesis, characterization and design for cancer cells nanotechnology-based targeting. *International Journal of Nanoscience and Nanotechnology* in press
- Jain PK, Huang X, El-Sayed IH, El-Sayed MA (2008) Noble metals on the nanoscale: Optical and photothermal properties and some applications in imaging, sensing, biology, and medicine. *Accounts of Chemical Research* **41**, 1578-1586
- Johnson SR, Evans SD, Brydson R (1998) Influence of a terminal functionality on the physical properties of surfactant-stabilized gold nanoparticles. *Langmuir* **14**, 6639-6647
- Link S, El-Sayed MA (1999) Size and temperature dependence of the plasmon absorption of colloidal gold nanoparticles. *The Journal of Physical Chemistry B* **103**, 4212-4217
- Mansoori GA (2005) *Principles of Nanotechnology: Molecular Based Study of Condensed Matter in Small Systems*, World Science Publishers Co., Hackensack, NJ, 341 pp
- Mansoori GA, George TF, Assoufid L, Zhang G (Eds) (2007) Molecular building blocks for nanotechnology: From diamondoids to nanoscale materials and applications. In: *Topics in Applied Physics* (Vol 109), Springer, NY, 341 pp
- Mansoori GA, Mohazzabi P, McCormack P, Jabbari S (2007) Nanotechnology in cancer prevention, detection and treatment: bright future lies ahead. *World Review of Science, Technology and Sustainable Development* **4**, 226-257
- Masters JR (2002) HeLa cells 50 years on: the good, the bad and the ugly. *Nature Reviews Cancer* **2**, 315-319
- Pan D, Turner JL, Wooley KL (2003) Folic acid-conjugated nanostructured materials designed for cancer cell targeting. *Chemical Communications (Cambridge)* **7**, 2400-2401
- Smith MB, March J (2007) *March's Advanced Organic Chemistry: Reactions, Mechanisms, and Structure* (6<sup>th</sup> Edn), John Wiley & Sons, NY, 550 pp
- Sudimack J, Lee RJ (2000) Targeted drug delivery via the folate-receptor. *Advanced Drug Delivery Review* **41**, 147-162
- Zhang Z, Zhou F, Lavernia EJ (2003) On the analysis of grain size in bulk nanocrystalline materials via X-ray diffraction. *Metallurgical and Materials Transactions A* **34**, 1349-1355
- Zharov VP, Galitovsky V, Viegas M (2003) Photothermal detection of local thermal effects during selective nanophotothermolysis. *Applied Physics Letters* **83**, 4897-4899